

April 2003

Studying top quark pair production at a linear collider with a program eett6f^{1,2}

Karol Kołodziej³

*Institute of Physics, University of Silesia
ul. Uniwersytecka 4, PL-40007 Katowice, Poland*

Abstract

Some features of a program **eett6f** for top quark pair production and decay into six fermions at linear colliders are discussed. Lowest order standard model predictions for cross sections of some six fermion channels and for the top quark decay width are confronted with the predictions obtained within a model with an anomalous Wtb coupling. The question of whether non doubly resonant background can easily be reduced by imposing kinematical cuts is addressed.

¹Presented at the Cracow Epiphany Conference on Heavy Flavors, Cracow, Poland, January 3–6, 2003.

²Work supported in part by the Polish State Committee for Scientific Research (KBN) under contract No. 2 P03B 045 23 and by European Commission's 5-th Framework contract HPRN-CT-2000-00149.

³E-mail: kolodzie@us.edu.pl

1 INTRODUCTION

As a top quark is the heaviest matter particle ever observed, with mass close to the energy scale of the electroweak symmetry breaking, investigation of its physical properties may give hints towards understanding physics beyond the Standard Model at higher energy scales. Therefore precise measurements, at a level of a few per mille, of the top quark properties and interactions will most certainly belong to the research program of any future e^+e^- linear collider [1]. In order to match that high precision level of the measurements, theoretical predictions should include radiative corrections.

As it has been shown in [2] and will be illustrated later in this lecture, effects caused by the off-shellness of the $t\bar{t}$ pair and off-resonance contributions may be important too, especially for measurements at the centre of mass system (c.m.s.) energies much above the $t\bar{t}$ threshold. As the t - and \bar{t} -quark of the reaction

$$e^+e^- \rightarrow t\bar{t} \quad (1)$$

almost immediately decay, predominantly into bW^+ and $\bar{b}W^-$, with the W^\pm boson decaying into a fermion pair, what one actually observes are 6 fermion reactions of the form

$$e^+e^- \rightarrow bf_1\bar{f}'_1\bar{b}f_2\bar{f}'_2, \quad (2)$$

where $f_1 = \nu_e, \nu_\mu, \nu_\tau, u, c$, $f_2 = e^-, \mu^-, \tau^-, d, s$ and f'_1, f'_2 are the corresponding weak isospin partners, $f'_1 = e^-, \mu^-, \tau^-, d, s$, $f'_2 = \nu_e, \nu_\mu, \nu_\tau, u, c$. For example, a pure electroweak (EW) reaction

$$e^+e^- \rightarrow b\nu_\mu\mu^+\bar{b}\mu^-\bar{\nu}_\mu \quad (3)$$

in unitary gauge receives contributions from 452 Feynman diagrams, neglecting the Higgs boson couplings to fermions lighter than b , while there are only two ‘signal’ diagrams contributing to reaction (2) in the double resonance approximation

$$e^+e^- \rightarrow \bar{t}^*t^* \rightarrow bf_1\bar{f}'_1\bar{b}f_2\bar{f}'_2 \quad (4)$$

at the same time.

In the present lecture, some features of the updated version of a computer program **eett6f** [2] that allows for computing cross sections of reactions (2) to the lowest order of the standard model (SM), with a complete set of the Feynman diagrams, will be discussed. The question of whether the non doubly resonant background can easily be reduced by imposing kinematical cuts will be addressed. Moreover, lowest order SM predictions for some six fermion channels of (2) and for the 3 particle top quark decay width will be confronted with the predictions obtained within a model with an anomalous Wtb coupling.

2 A PROGRAM

A computer program **eett6f** for calculating cross sections of 6 fermion reactions (2) relevant for a $t\bar{t}$ -pair production and decay at c.m.s. energies typical for linear colliders has been written in **FORTRAN 90** [3]. The program consists of 50 files including a `makefile`, all stored in one working directory. The user should specify the physical input parameters in a module

`inprms.f` and select a number of options in the main program `csee6f.f`. The options allow, among other, for calculation of the cross sections while switching on and off different subsets of the Feynman diagrams. It is also possible to calculate cross sections in two different narrow width approximations, for $t\bar{t}$ -quarks, or W^\pm -bosons. The program allows for taking into account both the EW and QCD lowest order contributions. Version 1 of the program allows for calculating both the total and differential cross sections of (2) at tree level of SM. Some anomalous effects beyond the SM that will be discussed later have been already implemented in the program. The program can be used as the Monte Carlo (MC) generator of unweighted events as well.

Matrix elements are calculated with the helicity amplitude method described in [4]. Phase space integrations are performed with the MC method. The most relevant peaks of the matrix element squared, related to the Breit-Wigner shape of the W, Z , Higgs and top quark resonances, and to the exchange of a massless photon, or gluon have to be mapped away. As it is not possible to find out a single parametrization of the 14-dimensional phase space which would allow to cover the whole resonance structure of the integrand, the program utilizes a multichannel MC approach.

Constant widths of unstable particles: the massive electroweak vector bosons, the Higgs boson and the top quark, are introduced through the complex mass parameters

$$\begin{aligned} M_V^2 &= m_V^2 - i m_V \Gamma_V, & V = W, Z, \\ M_H^2 &= m_H^2 - i m_H \Gamma_H, & M_t = m_t - i \Gamma_t / 2, \end{aligned} \quad (5)$$

which replace masses in the corresponding propagators,

$$\begin{aligned} \Delta_F^{\mu\nu}(q) &= \frac{-g^{\mu\nu} + q^\mu q^\nu / M_V^2}{q^2 - M_V^2}, \\ \Delta_F(q) &= \frac{1}{q^2 - M_H^2}, & S_F(q) = \frac{q + M_t}{q^2 - M_t^2}. \end{aligned} \quad (6)$$

Propagators of a photon and a gluon are taken in the Feynman gauge.

The EW mixing parameter may be defined either real or complex,

$$\sin^2 \theta_W = 1 - \frac{m_W^2}{m_Z^2}, \quad \text{or} \quad \sin^2 \theta_W = 1 - \frac{M_W^2}{M_Z^2}. \quad (7)$$

Performing substitution (6) both in the s - and t -channel Feynman diagrams and taking the complex electroweak mixing parameter of Eq. (7) leads to fulfilment of the Ward identities. As light fermion masses are not neglected, cross sections can be calculated without any kinematical cuts.

A number of checks of the program `eett6f` have been performed. The reader is referred to [3] for details.

In the present version of the program, an anomalous Wtb coupling has been implemented. The model describing departures of the Wtb interaction from the SM, caused by new fundamental interactions at high energies, can be specified in terms of the low energy effective lagrangian containing terms of dimension 6 [5]

$$\begin{aligned} L = \frac{g}{\sqrt{2}} & \left[W_\mu^- \bar{b} \gamma^\mu (f_1^- P_- + f_1^+ P_+) t \right. \\ & \left. - \frac{1}{m_W} \partial_\nu W_\mu^- \bar{b} \sigma^{\mu\nu} (f_2^- P_- + f_2^+ P_+) t \right] + \text{h.c.} \end{aligned} \quad (8)$$

In Eq. (8), P_{\pm} are chirality projectors given by $P_{\pm} = (1 \pm \gamma_5)/2$, $\sigma^{\mu\nu} = i(\gamma^{\mu}\gamma^{\nu} - \gamma^{\nu}\gamma^{\mu})/2$, the anomalous couplings f_1^{\pm} and f_2^{\pm} are assumed to be real, and W^- should be regarded as an effective vector field. The SM Wtb coupling is reproduced with $f_1^+ = f_2^- = f_2^+ = 0$ and f_1^- equal to the real Cabibbo-Kobayashi-Maskawa matrix element V_{tb} . According to the present experimental data, V_{tb} is very close to 1 [6] and f_1^+ is strongly constrained by the CLEO $b \rightarrow s\gamma$ data which give $f_1^+ \approx 0$ [7]. The couplings f_2^- and f_2^+ are at present only weakly constrained, see *e.g.* [8].

3 NUMERICAL RESULTS

In the present section, a sample of numerical results obtained with the current version of **eett6f** will be presented. The physical input parameters that are used are the same as in [2].

The energy dependence of the total cross sections of (3) is shown in Figure 1. The full lowest order cross section σ is plotted with the solid line, the signal cross section $\sigma_{\bar{t}^*t^*}$ with the dotted line, and the cross section in the narrow top width approximation, $\sigma_{\bar{t}t}$, with the dashed line. A comparison of the solid and dotted lines shows the effects of the off resonance background contributions to reaction (3), and a comparison of the dotted and dashed lines shows the effect of the off-mass-shell production of the $t\bar{t}$ -pair. Both effects are substantial, especially at higher energies. Therefore they should be taken into account in the future analysis of data.

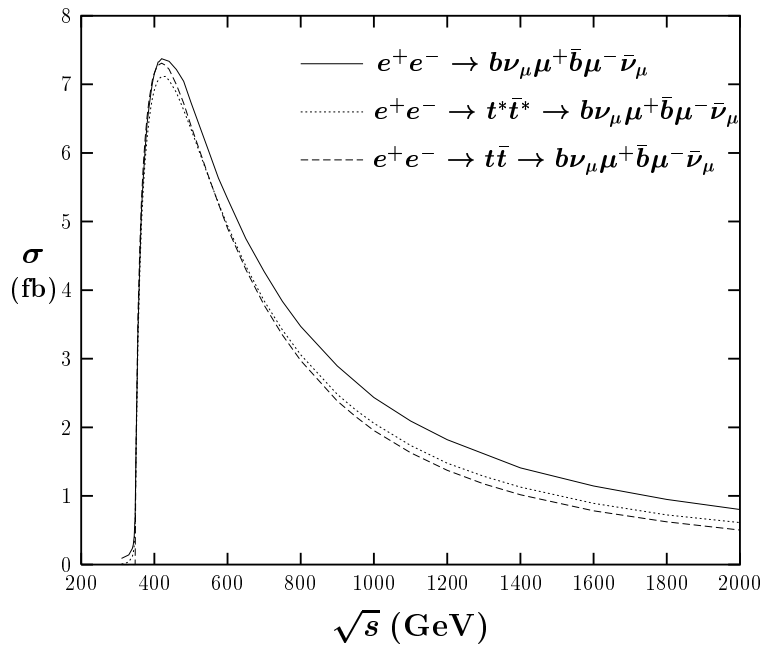


Figure 1: Total cross sections of $e^+e^- \rightarrow b\nu_{\mu}\mu^+\bar{b}\mu^-\bar{\nu}_{\mu}$ as functions of the c.m.s. energy.

The question arises, whether those big off resonance effects and background contributions can easily be reduced by imposing cuts. This issue will be preliminarily addressed below for one specific channel of reaction (2) by imposing the following cuts that are usually used in

literature

$$\begin{aligned}
\theta(l, \text{beam}) &> 5^\circ, & \theta(q, \text{beam}) &> 5^\circ, \\
\theta(l, l') &> 5^\circ, & \theta(l, q) &> 5^\circ, \\
E_l &> 10 \text{ GeV}, & E_q &> 10 \text{ GeV}, \\
m(q, q') &> 10 \text{ GeV},
\end{aligned} \tag{9}$$

where q, l denote quark and charged lepton, respectively.

Results for three differential cross sections: invariant mass distribution of a $\bar{b}d\bar{u}$ -quark triple and energy distributions of a b -quark and μ^+ of $e^+e^- \rightarrow b\nu_\mu\mu^+\bar{b}d\bar{u}$ at the c.m.s. energy of 500 GeV with cuts (9) have been compared against the corresponding results without cuts in Figs. 2–4. The solid histograms in Figs. 2–4 show the lowest order SM results obtained with the complete set of the Feynman diagrams, the dotted histograms show the contribution of the two $t\bar{t}$ signal diagrams and the dashed histograms have been obtained in the narrow top width approximation. The dotted histograms in Fig. 2 cannot be distinguished from the solid ones.

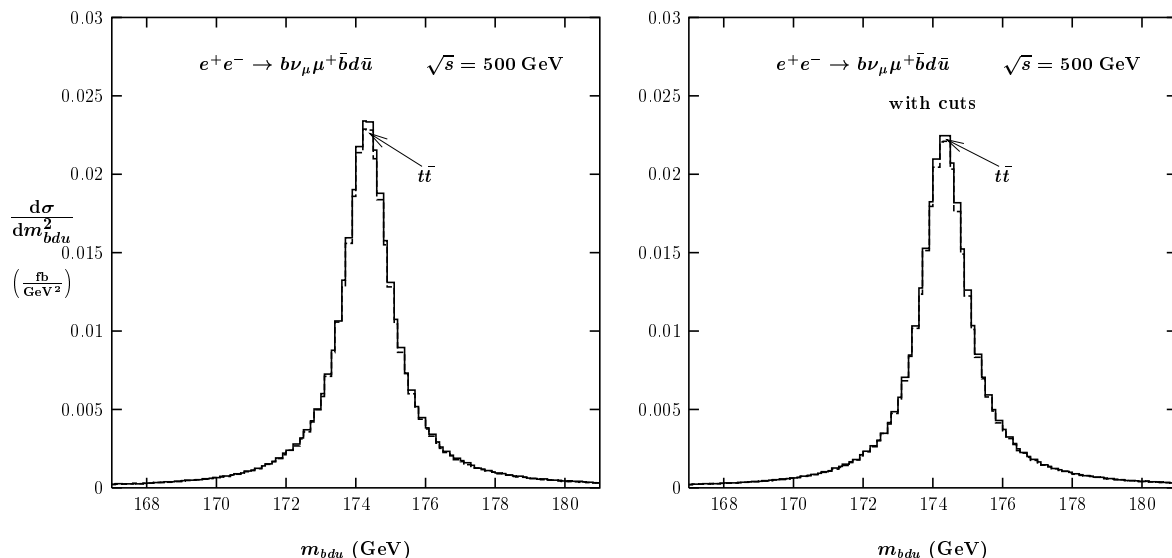


Figure 2: Invariant mass distributions of a $\bar{b}d\bar{u}$ -quark triple at $\sqrt{s} = 500$ GeV without cuts (left) and with cuts (right).

By comparing the plots on the left and right hand side of Figs. 2–4, one sees that, with cuts (9), the background and off resonance contributions are reduced to a similar extent as the top pair production signal itself. Of course, this somewhat naive analysis does not preclude existence of a set of cuts that would keep intensity of the signal and reduced the background at the same time, but finding this suitable set need not be a completely simple task at all.

`eet6f` gives also a possibility of looking at effects of the anomalous Wtb coupling defined by Eq. (8) that have been implemented in the program. Figs. 5 and 6 illustrate how the possible existence of an anomalous coupling f_2^+ may change angular and energy distributions of t -quark decay products in the rest frame of the top. The solid histograms show the SM results, while the dotted histograms represent results in presence of the anomalous Wtb coupling with $f_1^- = 1$, $f_1^+ = f_2^- = 0$ and $f_2^+ = 0.1$, both in Fig. 5 and 6. In Fig. 5, the well known fact from the literature that angular distribution of the charged lepton resulting from the decay $t \rightarrow b\mu^+\nu_\mu$ is the most efficient analyzer of the top-quark spin [9] is recollected. Solid histograms

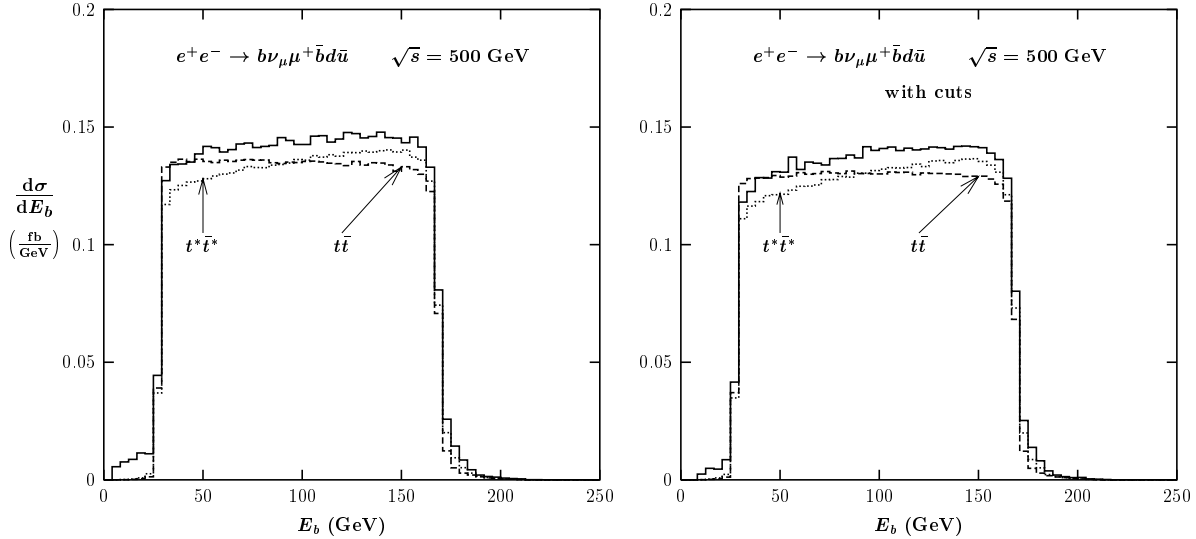


Figure 3: Energy distributions of a b -quark at $\sqrt{s} = 500$ GeV without cuts and with cuts.

in Fig. 5 clearly show proportionality of the angular distribution of μ^+ to $(1 + \cos \theta)$ if the spin of the decaying top-quark points in the positive direction of the quantization axis (spin up) and to $(1 - \cos \theta)$ if the spin of the decaying top-quark points in the negative direction of the quantization axis (spin down).

The angular and energy distributions of a b -quark and μ^+ resulting from the decay of t -quark produced in e^+e^- annihilation at $\sqrt{s} = 360$ GeV are plotted in Figs. 7 and 8. Again the solid histograms show SM results while the dotted, dashed and dashed-dotted histograms represent results in presence of the anomalous Wtb coupling. One sees that the flat histograms of Fig. 5 corresponding to decay of the unpolarized top quark have developed a slope due to the Lorentz boost from the rest frame of t -quark to the c.m.s. of e^+e^- . Similarly, how the Lorentz boost changes the energy distributions of the top decay products is illustrated in Fig. 8. It is interesting to note, how the relatively big effects arising if only a single anomalous coupling is nonzero, *i.e.* $f_2^+ = 0.1$ and $f_2^- = 0$ (dotted histograms), or $f_2^+ = 0$ and $f_2^- = 0.1$ (dashed histograms), are reduced by interference, if $f_2^+ = 0.1$ and $f_2^- = 0.1$ (dashed-dotted histograms).

4 SUMMARY AND OUTLOOK

Top quark pair production and decay into 6 fermions in e^+e^- annihilation at c.m.s. energies typical for linear colliders can be theoretically studied to the lowest order of SM with a program `eett6f`. A sample of results on selected channels of reaction (2) have been presented. It has been shown that, although the two $t\bar{t}$ signal diagrams dominate total cross sections even at c.m.s. energies much above the $t\bar{t}$ threshold, the effects related to off-mass-shell production of the $t\bar{t}$ -pair and the off resonance background may be relevant for the analysis of future precision data. It has been illustrated that these effects are not reduced by imposing typical cuts given by (9). Some extensions of the SM have been implemented in the program and results illustrating effects of the nonstandard Wtb coupling Eq. (8) have been shown.

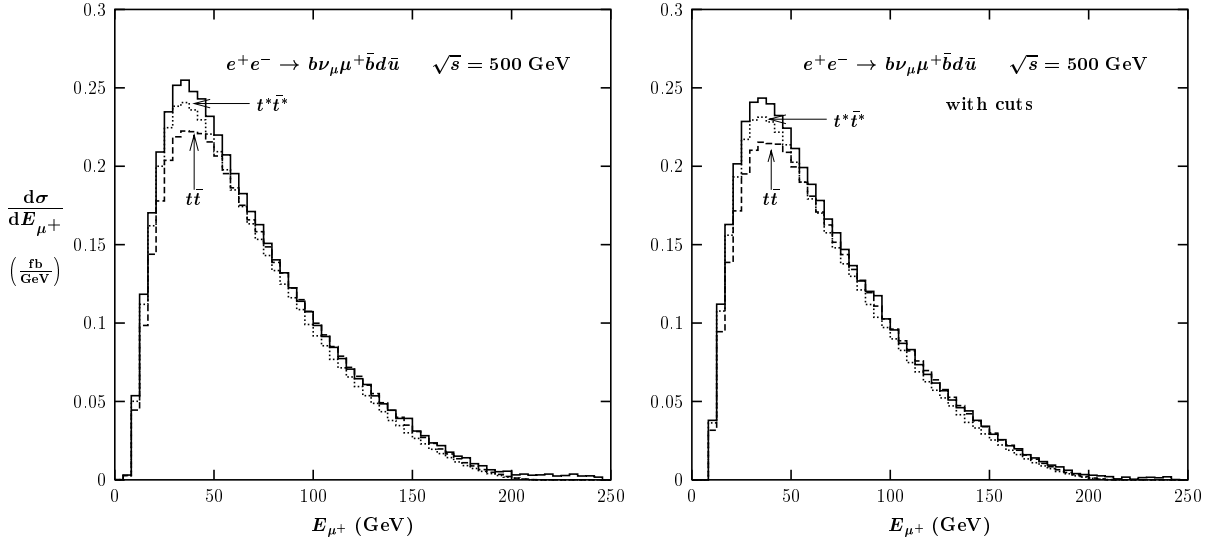


Figure 4: Energy distributions of a μ^+ at $\sqrt{s} = 500$ GeV without cuts and with cuts.

Work towards completing implementation of all the channels of (2) possible in the SM is underway. In order to match high precision of future experiments it is also required to implement higher order effects. As it is not feasible to calculate radiative corrections to the full set of Feynman diagrams that contribute to any specific channel of (2), it would be desirable to include higher order effects at least to the two signal diagrams. This approach would be justified by the fact that the total cross section of reactions (2) is dominated by the doubly resonant signal. Work in this direction is planned in collaboration with the Zeuthen–Bielefeld group [10].

References

- [1] TESLA Technical Design Report, Part III: Physics at an e^+e^- Linear Collider, edited by R.-D. Heuer, D. Miller, F. Richard, P.M. Zerwas, DESY 2001-011, ECFA 2001-209, TESLA Report 2001-23, TESLA-FEL 2001-05, March 2001, hep-ph/0106315; T. Abe *et al.*, American Linear Collider Working Group Collaboration, SLAC-R-570, *Resource book for Snowmass 2001*. K. Abe *et al.*, hep-ph/0109166.
- [2] K. Kołodziej, Eur. Phys. J. **C23**, 471 (2002);
A. Biernacik, K. Kołodziej, Nucl. Phys. B (Proc. Suppl) **116**, 33 (2003), hep-ph/0210405.
- [3] K. Kołodziej, Comput. Phys. Commun. **151**, 339 (2003), hep-ph/0210199.
- [4] K. Kołodziej, M. Zrałek, Phys. Rev. **D43**, 3619 (1991);
F. Jegerlehner, K. Kołodziej, Eur. Phys. J. **C12**, 77 (2000).
- [5] G.L. Kane, G.A. Ladinsky, C.-P. Yuan, Phys. Rev. **D45**, 124, (1992);
E. Boos, M. Dubinin, M. Sachwitz, H.J. Schreiber, Eur. Phys. J. **C16**, 269 (2000);
B. Grzadkowski, Z. Hioki, Phys. Lett. **B476**, 87 (2000).
- [6] K. Hagiwara *et al.*, Phys. Rev. **D66**, 010001 (2002).

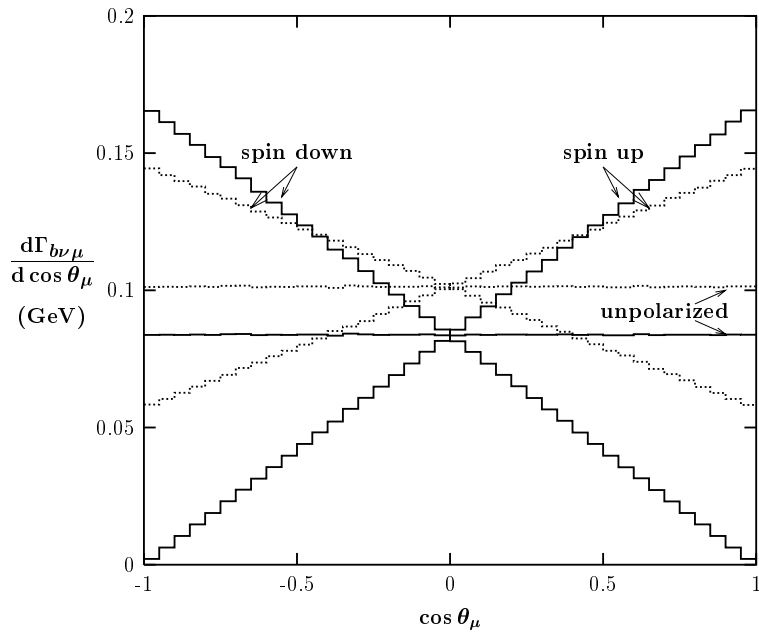


Figure 5: Angular distributions of a top quark decay products in the top rest frame.

- [7] M. Alam, *et.al.*, CLEO Collaboration, Phys. Rev. Lett. **74**, 2885 (1995).
- [8] K. Whisnant, J.M. Yang, B.-L. Young, X. Zhang, Phys. Rev. **D56**, 467 (1997).
- [9] M. Jeżabek, J.H. Kühn, Nucl.Phys. **B320**, 20 (1989).
- [10] J. Fleischer, A. Leike, T. Riemann, A. Werthenbach, hep-ph/0302259.

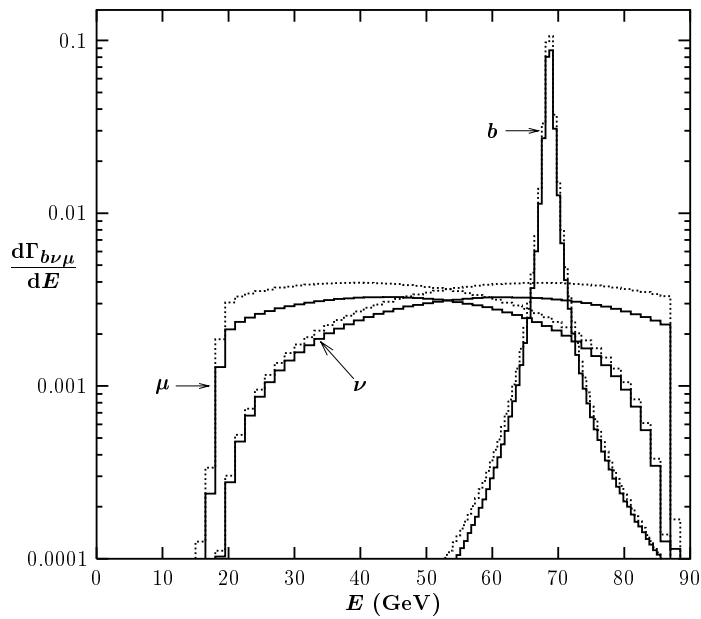


Figure 6: Energy distributions of a top quark decay products in the top rest frame.

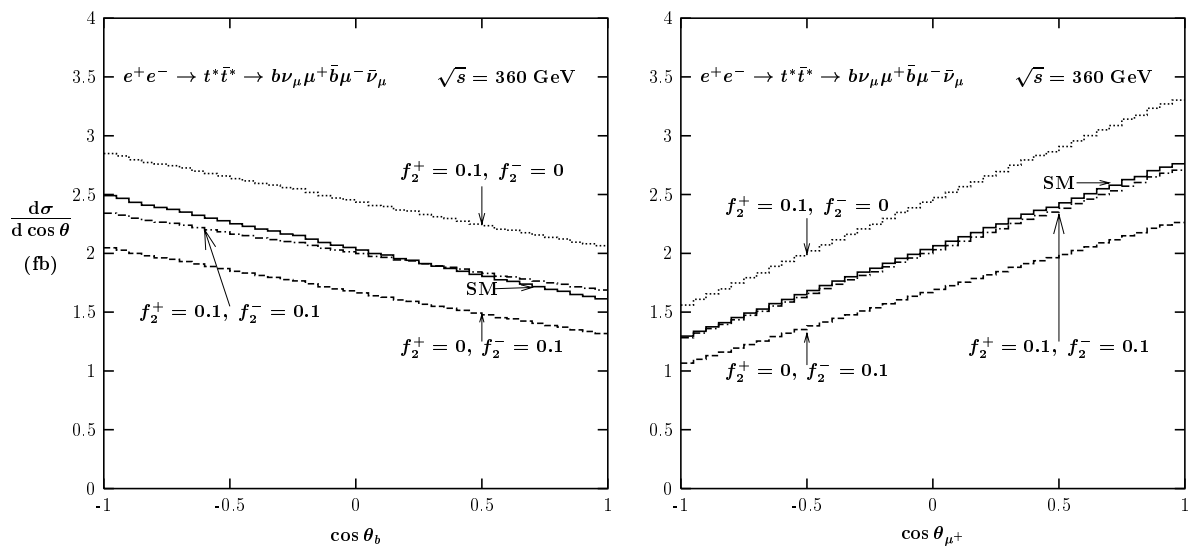


Figure 7: Angular distributions of a b -quark (left) and μ^+ (right) at $\sqrt{s} = 360$ GeV.

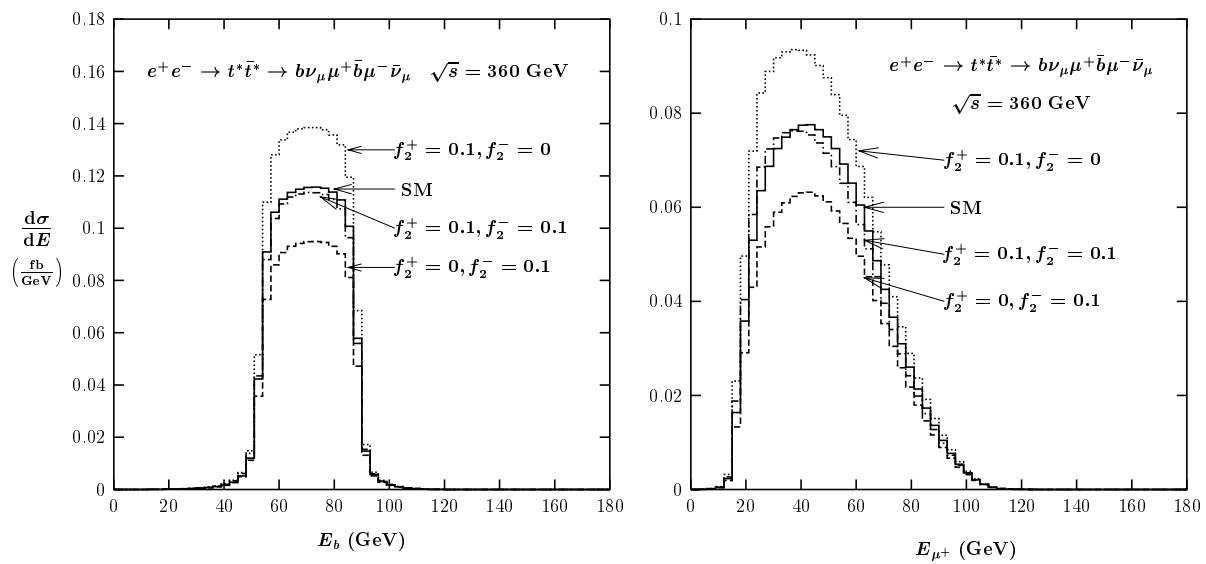


Figure 8: Energy distributions of a b -quark (left) and μ^+ (right) at $\sqrt{s} = 360$ GeV.

